Theory and Practice of Reversing Control on Multiply-Articulated Vehicles

Journal:	*Part D: Journal of Automobile Engineering*
Manuscript ID:	JAUTO-14-0454.R2
Manuscript Type:	Original Article
Date Submitted by the Author:	22-Jun-2015
Complete List of Authors:	Rimmer, Amy; University of Cambridge, Department of Engineering Cebon, David; University of Cambridge, Engineering
Keywords:	vehicle control systems, commercial vehicles, goods vehicles/ trucks, heavy vehicle systems, intelligent vehicles
Abstract:	A path-tracking controller is presented for automating the reversing of multiply-articulated vehicles. This uses a state feedback approach and steers the wheels of the front axle to ensure the rearmost vehicle unit tracks a specified path. Linear closed-loop analysis is performed and shows that the controller is stable for vehicles with up to six trailers. The controller is implemented on three full-size, experimental heavy vehicles: a 'Tractor-Semitrailer', 'B-double' and 'B-triple' which have one, two and three trailers respectively. Experimental results are presented and the controller performance is evaluated. All test vehicles were able to track paths to within 400mm of the desired path.

Theory and Practice of Reversing Control on Multiply-Articulated Vehicles

Submitted to IMechE Part D Journal of Automobile Engineering in December 2014

Authors: Rimmer, AJ; Cebon, D*

* Corresponding author: dc@eng.cam.ac.uk, Cambridge University Engineering Department, Trumpington Street, Cambridge, CB2 1PZ, United Kingdom

Abstract

A path-tracking controller is presented for automating the reversing of multiply-articulated vehicles. This uses a state feedback approach and steers the wheels of the front axle to ensure the rearmost vehicle unit tracks a specified path. Linear closed-loop analysis is performed and shows that the controller is stable for vehicles with up to six trailers. The controller is implemented on three full-size, experimental heavy vehicles: a 'Tractor-Semitrailer', 'B-double' and 'B-triple' which have one, two and three trailers respectively. Experimental results are presented and the controller performance is evaluated. All test vehicles were able to track paths to within 400mm of the desired path.

Keywords: reversing, articulated vehicle, path-tracking, control, trailer

1 Introduction

Using longer heavy vehicles can give reductions in fuel consumption (up to 30%), road wear (40%) and the number of heavy vehicles on the roads (44%) (1, 2). Multiply-

articulated heavy vehicles are used in Scandinavian countries, the Netherlands, much of the USA, South Africa, Canada and Australia.

Examples of multiply-articulated vehicles found in the road-freight industry include the 'B-double' and the 'B-triple' (Figure 1(b) and (c)), which have two and three trailers respectively. These are collectively known as 'B-trains', which are vehicles with a tractor unit at the front, a semitrailer at the rear and a number of 'B-trailers' in between. A 'B-trailer' is a special trailer with an additional fifth wheel coupling which enables connection of another semitrailer. A more conventional, shorter heavy vehicle is a 'Tractor-Semitrailer' (Figure 1(a)), which has one trailer.

Reversing multiply-articulated heavy vehicles is challenging for professional drivers and tends to be avoided where possible (3). Therefore, a semi-autonomous system for reversing these vehicles would prove useful. In order to introduce such a system, a path-tracking controller for reversing multiply-articulated vehicles is required.

The problem of reversing an articulated vehicle to follow a desired path has been investigated in the literature. There are examples of reversing controllers for the multiple-trailer case (4-12), but there is a lack of formal controller performance evaluation. No previous research has included the tyre scrubbing characteristics of multiple-axle trailers on heavy vehicles. The most significant shortcoming in the literature, however, is that none of the approaches have been tested on a full-size heavy vehicle.

This paper aims to address these shortcomings by conducting field tests on three full-size experimental heavy vehicles, as shown in Figure 1. A state feedback path-tracking controller (13) is presented for the general n-trailer vehicle. Theoretical analysis is

conducted on B-train vehicle combinations. The controller is tested on a Tractor-Semitrailer, a B-double and a B-triple, which have one, two and three trailers respectively. Test results are presented and the performance of the path-tracking controller on all three test vehicles is evaluated. The work presented here is part of a larger study investigating reversing of multiply-articulated vehicles (13).

2 Control Theory

The objective of the path-tracking controller is to make a specified axle on the rear trailer follow a desired path (13). In Figure 2, which shows a schematic of the vehicle for the two-trailer case, this means point V_A should follow the desired path. If the rear trailer has multiple axles, Winkler's approach (14) can be used to calculate the 'equivalent' trailer wheelbase, shown as l on Figure 2, which is then used to define the position of V_A. Details of the equivalent wheelbase calculations can be found in (13).

2.1 Performance Criteria

In order to make a formal assessment of a path-tracking controller, a set of performance criteria was defined:

(i) The 'path offset' is the distance of the equivalent axle on the rear trailer from the specified path. Minimising 'path offset' was the primary control objective. RMS and maximum values were evaluated.

(ii) The 'steer integral' is the integral of absolute steer angle with respect to distance, $\int |\delta| \, ds$. This is a measure of steer effort.

(iii) The 'RMS steer rate'. This has a limit based on the steering actuation hardware of the vehicle.

(iv) The 'swept path' of the vehicle. The area the vehicle sweeps through as it manoeuvres the path was recorded and the width of this area relative to the path was calculated. RMS and maximum values were evaluated.

2.2 *Vehicle Modelling*

In order to develop a reversing controller, it was necessary to derive a mathematical model of a multiply-articulated heavy vehicle. A general dynamic vehicle model was implemented in MATLAB®. This modelled lateral tyre forces and inertial forces on the vehicle and was used to calculate yaw-sideslip motion. This model was an extension of the standard bicycle model (15) with an arbitrary number of trailers (n), each having any number of axles. By appropriate choice of parameters, this general model can be used to model the low-speed behaviour of essentially any multiply-articulated vehicle. A schematic diagram of the model is shown in Figure 2 for the two-trailer case (n = 2).

Assumptions

The following was assumed when deriving the model:

(i) The longitudinal velocity of the tractor unit is constant

(ii) Yaw and sideslip motion only included; the effects of vehicle roll and pitch are neglected

(iii) The effects of lateral load transfer are neglected

(iv) The front axle of the tractor unit has perfect Ackerman geometry

(v) No sensor noise or other sensor imperfections

(vi) No saturation or rate limits

(vii) Each axle can be modelled by a single wheel, whose lateral tyre forces are calculated using an appropriate tyre model.

Tyre Modelling

A nonlinear tyre model (16) suitable for truck tyres (from (17)) was used to calculate the lateral tyre forces. For a given slip angle, α, the lateral tyre force (F) can be calculated:

$$\frac{F}{\mu Z} = \begin{cases} \frac{\bar{C}}{\mu}\alpha - \frac{\bar{C}^2}{3\mu^2}|\alpha|\alpha + \frac{\bar{C}^3}{27\mu^3}\alpha^3 & |\alpha| < \frac{3\mu}{\bar{C}} \\ \text{sign}(\alpha) & \end{cases} \quad (1)$$

$$\bar{C} = C_1 + C_2 Z \quad (2)$$

Here, Z is the vertical load at the wheel; C_1 and C_2 are tyre model coefficients and μ is the coefficient of friction between the tyre and the road.

The vertical tyre loads were calculated using static analyses of the vehicles. For a trailer with multiple axles, it was assumed that all tyres in the axle group carried equal vertical loads. The tyre parameters are shown in Table 1 (as used in (18)).

Vehicle Model Derivation

For the entire vehicle, the state vector, $\mathbf{z}$, was defined as:

$$\mathbf{z} = \begin{bmatrix} v_1 & \Omega_1 & \Gamma_j & \dot{\Gamma}_j \end{bmatrix}^T, \ \dot{\mathbf{z}} = \begin{bmatrix} \dot{v}_1 & \dot{\Omega}_1 & \dot{\Gamma}_j & \ddot{\Gamma}_j \end{bmatrix}^T, \ j = 1, 2 \ldots n \quad (3)$$

Here, v_1 and Ω_1 are the lateral velocity and yaw rate at the centre of gravity of the tractor unit, and Γ_j is the articulation angle between the j^{th} and $j+1^{th}$ vehicle units, see Figure 2.

For each vehicle unit, velocities and accelerations at the centre of gravity can be calculated in terms of the state vector using kinematics. The slip angles for each wheel can then be calculated, and the lateral tyre forces can be calculated from the slip angles using Equation (1). The resulting equations of motion for the vehicle are shown in the Appendix.

The equations of motion can be rearranged into the following form:

$$f_m(\delta, \mathbf{z}, \dot{\mathbf{z}}) = 0 \quad (4)$$

$$\dot{\mathbf{z}} = f_d(\delta, \mathbf{z}) \quad (5)$$

Here, δ is the front axle steer angle of the tractor unit and f_m is a nonlinear function containing all equations of motion from (A.1) to (A.5) from the Appendix and equating all articulation angle rates from the state vector and its derivative. f_d is the rearranged nonlinear function to be used with an Ordinary Differential Equation (ODE) solver.

Vehicle parameters for common heavy vehicle units are shown in Table 1 and Figure 2. Geometries, masses and inertias were obtained from previous research (18, 19) and measured from the Cambridge Vehicle Dynamics Consortium's test vehicles (20).

Table 1: Vehicle and tyre model parameters

Parameter			Tractor	Denby 'Extra' B-trailer	CVDC 'Modular Vehicle' B-trailer	Semitrailer
Definition	Symbol	Unit				
Front axle or hitch to centre of gravity	a	m	1.13	5.00	7	6.00
First rear axle to centre of gravity	b	m	2.58	2.90	2.32	0.420
First rear axle to hitch	c	m	-0.16	0.64	0.81	4.8
Number of axles	n_a		2	2	2	3
Axle spacing	e	m	-	1.80	1.46	1.30
Front overhang	fo	m	1.40	1.80	1.94	1.50
Rear overhang	ro	m	1.25	2.50	2.33	5.00
Vehicle width (excluding mirrors)	d	m	2.40	2.50	2.5	2.38
Mass	m	kg	6988	10500	15000	8800
Yaw Inertia	I	kgm^2	42147	156860	156860	156860

Tyre Cornering Coefficient	C_1	1/rad	-8.78	-6.28		
Tyre Curvature Coefficient	C_2	1/Nrad	494e-5	3.4e-6		
Coefficient of friction	μ	-	0.8			
Equivalent wheelbase	l	m	-	-	-	7.85

Linearisation

The vehicle model was linearised for the straight line case (all states set to zero) using Jacobian linearisation (21). Equation (4) can be expressed in linear form for small variations from the equilibrium position:

$$[\mathbf{M}]\dot{\boldsymbol{z}}+[\mathbf{N}]\boldsymbol{z}+[\mathbf{H}]\delta = 0 \quad (6)$$

where $[\mathbf{M}] = \frac{\partial f_m}{\partial \dot{\boldsymbol{z}}}$, $[\mathbf{N}] = \frac{\partial f_m}{\partial \mathbf{z}}$ and $[\mathbf{H}] = \frac{\partial f_m}{\partial \delta}$

2.3 Path-Tracking Controller

A state feedback controller was used for the path-tracking control problem. It included feedback control on articulation angles, lateral offset and heading error at the equivalent axle on the rear trailer (i.e. point V_A). Some features of the controller are illustrated in Figure 3 for a two-trailer vehicle.

The steer angle was calculated as follows:

$$\delta = \delta_e+K_{y_a}\, y_a+K_{\theta_a}\left(\theta_p-\theta_t\right)+\sum_{j=1}^{n} K_{\Gamma_j}\left(\Gamma_{e_j}-\Gamma_j\right) \quad (7)$$

Here, y_a is the lateral offset from the equivalent axle to the path. θ_t is the heading of the rear trailer and θ_p is the heading of the path. Γ_{e_j} is the j^{th} equilibrium articulation angle and δ_e is the equilibrium steer angle which are all calculated from the steady-state value corresponding to the current curvature of the path. K_{y_a}, K_{θ_a} and K_{Γ_j} are the controller gains corresponding to the axle offset, heading error, and j^{th} articulation angle respectively.

When articulated vehicles travel in reverse, it takes some distance for the steering at the front of the vehicle to take effect at the rear trailer. A 'look-ahead' approach was used to compensate for this delay. Instead of calculating the path curvature at the point where the axle offset is measured, P_A on Figure 3, the curvature was calculated at point P_L a certain 'look-ahead' distance (L_{LA}) along the path. This curvature was then used to calculate the equilibrium steer angle and articulation angles used in the controller. The 'look-ahead' distance allows some distance for the vehicle to reposition if the path curvature is changing, but it makes no difference to the steady-state performance.

For an n-trailer vehicle, the state feedback controller has n+3 parameters to tune: lateral offset gain (K_{y_a}), heading offset gain (K_{θ_a}), n articulation angle gains (K_{Γ_j}), and the 'look-ahead' distance (L_{LA}). The control loop in Figure 4 shows the measurement of the lateral and heading offsets at the equivalent axle of the rear trailer and the calculation of the equilibrium articulation angles corresponding to the path curvature. Proportional gains are applied to all errors (lateral offset, heading offset and articulation angle error) and added to the corresponding equilibrium steer angle.

2.4 Controller Tuning

Linear Analysis

Linear control analysis was performed to assist with controller gain tuning. For simplicity, this analysis was carried out for small perturbations from a straight line, which was sufficient to capture the closed-loop stability characteristics of the system.

In order to represent the position of the vehicle in linear form, two observer states were added to the linear vehicle model; the lateral position of the tractor unit CoG (y_1) and the heading of the tractor unit (θ_1). These additional states were calculated as follows:

$$\dot{\theta}_1 = \Omega_1 \tag{8}$$

$$\dot{y}_1 = v_1 + u_1\theta_1 \tag{9}$$

where u_1 is the longitudinal speed of the tractor unit.

Equation (6) can be extended to include the additional states:

$$[\mathbf{M}_a]\dot{\boldsymbol{z}}_a + [\mathbf{N}_a]\boldsymbol{z}_a + [\mathbf{H}_a]\delta = 0 \tag{10}$$

Here, $\boldsymbol{z}_a$ is the state vector with two additional states: $\boldsymbol{z}_a = \left[\boldsymbol{z}^{\mathrm{T}} \quad y_1 \quad \theta_1\right]^{\mathrm{T}}$. $[\mathbf{M}_a]$ and $[\mathbf{N}_a]$ are modified versions of $[\mathbf{M}]$ and $[\mathbf{N}]$ which implement Equations (8) and (9). $[\mathbf{H}_a]$ is simply $[\mathbf{H} \quad 0 \quad 0]^T$ as the new states are not directly dependent on tractor unit steer angle.

The state feedback controller (Equation (7)) was linearised into the form:

$$\delta = [\mathbf{K}]\boldsymbol{z}_a \tag{11}$$

Where $[\mathbf{K}]$ is a gain matrix:

$$[\mathbf{K}]=\begin{bmatrix} 0 \\ 0 \\ -K_{y_a}(h_2+\ldots+h_n+l)-K_1-K_{\theta_a} \\ \vdots \\ -K_{y_a}l-K_n-K_{\theta_a} \\ 0 \\ \vdots \\ 0 \\ K_{y_a} \\ -K_{y_a}(b_1+c_1+h_2+\ldots+h_n+l)-K_{\theta_a} \end{bmatrix}^T \quad (12)$$

Here, b_1 and c_1 are centre of gravity to rear axle and rear axle to hitch point distances on the tractor unit (as shown on Figure 2) and h_i is the hitch to hitch distance of the i^{th} vehicle unit.

For the linearised model, the closed-loop system can be written as:

$$\dot{\mathbf{z}}_\mathbf{a} = [\mathbf{A}]\mathbf{z}_\mathbf{a} \quad (13)$$

where

$$[\mathbf{A}] = -[\mathbf{M}_a]^{-1}([\mathbf{N}_a]+[\mathbf{H}_a][\mathbf{K}]) \quad (14)$$

The eigenvalues of $[\mathbf{A}]$ can be used to determine the stability characteristics of the closed-loop response. The damping ratio for an eigenvalue is defined as (21):

$$\zeta = -\frac{\mathrm{Re}\{\mathrm{eig}([\mathbf{A}])\}}{|\mathrm{eig}([\mathbf{A}])|} \quad \text{for} \quad \mathrm{Re}\{\mathrm{eig}([\mathbf{A}])\} \le 0 \quad (15)$$

For a general n-trailer vehicle, the number of eigenvalues will equal the number of model states ($2n$+4). The eigenvalue with the lowest damping ratio was chosen for analysis because this will dominate the system response characteristics.

Controller Gain Selection

An LQR (Linear Quadratic Regulator) approach (22) has been used before to tune similar controllers (23, 24). This is an optimal control technique which calculates the control input sequence to minimise a given cost function. For the path-tracking controller, the cost function was defined as:

$$J = \int_0^\infty \left(w y_a^2 + \delta^2\right) dt \tag{16}$$

where w represents a weighting which can be used to tune how much emphasis is placed on the path offset of the equivalent axle on the rear trailer versus the steering effort.

The linear equivalent of Equation (16) was derived and a Ricatti equation was formed for the quadratic optimisation problem and solved numerically in MATLAB® (this was done offline). The optimum control action was calculated in terms of the state vector and expressed as gain matrix [**K**].

From the LQR gain matrix, the equivalent gains for the state feedback controller (K_{y_a}, K_{θ_a}, etc.) were calculated analytically using the vehicle geometry. This was done by defining a relationship between the equivalent axle on the rear trailer and the tractor unit for the heading and lateral offsets. The relationship was evaluated in matrix form:

$$\boldsymbol{z_a} = [\mathbf{T}]\boldsymbol{z_v} \tag{17}$$

Here, [**T**] is a co-ordinate transformation matrix, purely based on the vehicle geometry, which converts the location states on the tractor unit to those on the last trailer. $\boldsymbol{z_v}$ is the state vector with two additional states: $\boldsymbol{z_v} = [\boldsymbol{z}^T \quad y_a \quad \theta_t]^T$

This meant the equivalent gains could be calculated simply by multiplying the gain matrix generated from the LQR calculation by the co-ordinate transformation matrix.

$$[\mathbf{K_{SF}}] = [\mathbf{K}][\mathbf{T}] \tag{18}$$

where $[\mathbf{K_{SF}}] = [0 \quad 0 \quad K_{\Gamma_1} \quad \dots \quad K_{\Gamma_n} \quad 0 \quad \dots \quad 0 \quad K_y \quad K_\theta]$

Another parameter which required tuning was the 'look-ahead' distance (L_{LA}) for the state feedback controller. The 'look-ahead' distance was calculated using linear analysis for the articulation angle control loop (with desired last articulation angle as the input and last articulation angle as the output). The closed-loop system was defined with the articulation angle gains (K_{Γ_j}) calculated for the state feedback controller for a specified weighting (w). The closed-loop frequency response was calculated and the phase was divided by the frequency to give a time between the demanded articulation angle and the actual articulation angle. For a conventional stable system, this time would be negative, indicating a time delay.

The maximum delay (most negative time) was selected to calculate the 'look-ahead' distance parameter. During the simulation, the 'look-ahead' distance was computed online by multiplying the maximum time delay by the trailer speed. This was necessary because the tractor unit has constant longitudinal speed but the longitudinal speed of the rear trailer varies depending on the manoeuvre.

The controller gains are shown in Table 2 for an LQR weighting of 5 for a Tractor-Semitrailer, B-double and B-triple. These gains correspond to the vehicle model parameters in Table 1.

Table 2: Controller gains used in implementation on test vehicles

Weighting (w)	K_{θ_a}	K_{y_a}	K_{Γ_1}	K_{Γ_2}	K_{Γ_3}	L_{LA}

Tractor-Semitrailer	11.2	2.24	3.90	-	-	1.09
B-double	-21.0	-2.24	4.33	-17.1	-	2.77
B-triple	-31.0	2.24	4.75	-22.5	50.0	5.82

2.5 Closed-Loop Stability of B-trains

The linear analysis and the LQR tuning approach were used to develop linear models of the closed-loop system for B-train vehicles with various numbers of trailers, starting with the Tractor-Semitrailer, the B-double and so on. The LQR gains for each vehicle combination were computed and the lowest damping ratio of the closed loop poles was calculated for weightings, *w*, ranging from 0.1 to 10.

Figure 5 shows the damping ratio against controller weighting (*w*) for B-trains of up to six trailers. This shows that it is not possible to stably control a B-train with more than six trailers using this method. It also shows the damping ratio decreases as the number of vehicle units increases, as expected.

3 Controller Implementation

The path-tracking controller was implemented on a Tractor-Semitrailer, a B-double and a B-triple, shown in Figure 1. Most of the hardware was mounted on the tractor unit and the rear trailer (tanker), which were used in all three vehicle combinations. In this section, the hardware is explained in the context of the B-double test vehicle.

3.1 Test Equipment

Figure 6 shows a schematic of the test hardware including the sensors, actuators and computers on the vehicle, along with their approximate locations and connections. A CAN bus (Controller Area Network) using the ISO 11898 protocol was used to communicate digital signals between sensors on each vehicle unit and the 'global controller' (shown as the 'xPC' block). The global controller was operated using a laptop, connected via Ethernet.

A string potentiometer was used to measure the steer angle of the tractor unit's front wheels. The sensor was mounted to the underside of the chassis and the string was attached to the front left steering radius arm. The articulation angles were measured using specially modified kingpins, which have angle sensors mounted on them, made by V.S.E. (25, 26). All analogue signals were low-pass filtered and digitised, using analogue-to-digital converters (ADCs), and transmitted over the CAN bus to the controller. The zero positions of the string pot and articulation angle sensors were updated at the start of each test session to remove small signal offsets due to temperature and other drift. In the case of the B-triple, one further articulation angle sensor was used at the third hitch point.

A vehicle-based Oxford Technical Solutions (OxTS) RT3022 (GNSS and inertial sensor) (27) was used, with a base station and dual antennas, to measure position. The RT3022 was placed on the roof of the second trailer (tanker). The RT3022 signals were transmitted to the global controller using a CAN bus. The offset between the heading of the RT3022 and the heading of the trailer was measured at the start of each test session by driving in a straight line and determining the difference between the heading calculated from the position and the measured heading.

The quoted accuracies for the RT3022 in the configuration used in these experiments are 200mm for position and 0.1° for heading (27). The measured accuracies were around 40mm for latitude and longitude and 0.08° for heading. Line-tracking cameras were used to confirm the use of the RT3022 for assessing controller performance (see (13) for more details).

An Anthony Best Dynamics SR30 steering robot (28) was attached to the steering column (in place of the steering wheel) and used to actuate the demanded hand wheel angle. The robot was set to follow an external demand from the global controller via the CAN bus. The path-tracking controller presented in Section 2.3 was used to determine the front axle steer angle of the tractor unit, required to track a path. The relationship between the hand wheel and the road wheel was measured, stored in a lookup table, and used to generate the hand wheel angle from the desired front axle steer angle.

3.2 Global Controller

The control algorithms were implemented in real-time using the MATLAB® 'xPC target' toolbox. The global controller consisted of an 'xPC unit' which was a 500MHz PC with the hard drive removed, set up to boot from a floppy disc drive. It had Softing AC2-PCI dual CAN bus cards in the PCI slots.

The global controller code was written in the MATLAB® block diagram code environment, Simulink, which could then be automatically compiled and downloaded onto the xPC unit. This compilation was done using the Simulink Coder (formerly known as 'Real Time Workshop') to generate the C code and using the Microsoft Visual Studio C compiler to create an executable file.

A block diagram highlighting the main features of the global controller software is shown in Figure 7. The global position and heading of the equivalent axle on the rear trailer were calculated using the RT3022 measurements and its known location on the vehicle. At the start of each run, a path was set up to start in alignment with the position and heading of the equivalent axle on the rear trailer. The offsets from the path were then calculated for the equivalent axle and fed into the controller, along with articulation angles. The desired front axle steer angle was saturated with the known tractor steer limits and rate limited according to the vehicle speed, to prevent any dry steering when the vehicle was stationary. An overall rate limit was also imposed to prevent the demand angle rate exceeding the steering robot's range. The demand was converted to hand wheel angle and sent to the steering robot.

All measured and computed quantities were logged. The code ran at a frequency of 100Hz, which was compatible with all the hardware used and was sufficient to meet the bandwidth requirements of the controller.

The controller presented in Section 2 requires knowledge of the steady-state cornering equilibrium states (including front axle steer angle, δ_e, and articulation angles, Γ_{e_j}). These were measured at the start of each testing day. It was thought that using a set of equilibrium values measured from the vehicle would give better performance than simulated values, particularly in steady-state cornering (13). The reason for measuring the equilibrium states at the start of each day was due to the nonlinear tyre scrubbing behaviours of multiple-axle trailers. Nonlinear tyre properties can be affected by changes in temperature, humidity and other features of the surface that can vary from day to day (16). A test procedure was created to efficiently obtain the vehicle

equilibrium states by setting the steering robot to various steer angles and measuring the subsequent vehicle motion.

4 Field Tests

Lane change and roundabout paths, shown in Figure 8 and Figure 9 respectively, were used as desired paths for all three test vehicles. The roundabout path had a radius of 10m and both paths had continuous second derivative of curvature. The paths were designed to ensure the vehicles could negotiate the paths without violating the steer rate limits (see (13) for details).

An intermediate value of the LQR weighting ('*w*' in Equation 14) of 5 was used to tune the controller gains for all vehicles, shown in Table 2 (see (13) for a detailed discussion of the effect of this parameter). Three repeat tests were performed for each test configuration (path type and vehicle combination). The results were found to be repeatable apart from small random errors (see (13)) and so they were averaged with respect to distance.

All tests were conducted with the tractor unit travelling at -1m/s, starting from stationary. The effects of varying tractor unit speed were analysed and found to be negligible. It was possible to stop the vehicles part-way through a manoeuvre and continue without issue.

4.1 Experimental Results

The measured equivalent axle positions of all three test vehicles are shown in Figure 8 and Figure 9 for the lane change and roundabout manoeuvres respectively. This shows

the B-triple has a small, but noticable devation from the desired path, while the B-double and Tractor-Semitrailer track the path almost exactly.

The experimental results for all three vehicles are shown in Figure 10 for the lane change manoeuvre for (a) offsets of the equivalent axle on the rear trailer, (b) steer angles, (c) heading offsets of the equivalent axle, and (d)-(f) articulation angles. The last (n^{th}) articulation angles (Figure 10 (d)) are very similar for all vehicles, as expected. The penultimate (n-1^{th}) articulation angles (Figure 10 (e)) show similar trends between the B-double and B-triple vehicles.

The offsets of the equivalent axle on the rear trailer increase with the number of trailers (n) but still show good performance in all cases: less than 350mm offset for the B-triple, 120mm for the B-double and 60mm for the Tractor-Semitrailer. The heading offsets also increase with the number of trailers (n) but they are all less than 2 degrees in magnitude. The steer angles are much larger for the B-triple than the Tractor-Semitrailer and are closely related to the first articulation angle of each vehicle. The Tractor-Semitrailer settles out of the manoeuvre more quickly than the B-triple, because it is much shorter and it takes much less time to reach steady state.

Results for the roundabout manoeuvre are shown in Figure 11 and show similar trends to the lane change manoeuvre with slightly larger offsets (up to 400mm for the B-triple). There is strong agreement between all vehicles for the last and penultimate articulation angles for this manoeuvre (Figure 11 (d) and (e)).

A significant feature of these experimental results is the presence of small-amplitude oscillations (seen in the equivalent axle offsets and steer angles). The oscillations had an amplitude of approximately 50-200mm, which is less than a truck tyre width

(approximately 400mm). The amplitude of the oscillations increased with the number of trailers. All closed-loop experimental results from this research showed this phenomenon, which is particularly noticeable in steady-state parts of manoeuvres. A thorough investigation into the root cause of these oscillations was conducted in (13). It was found that a closed-loop system pole was being driven by lateral tyre force disturbances (probably caused by cross-slope on the rough test track surface), with propagation delays between axles. With some retuning of controller gains, it was possible to reduce the size of the oscillations slightly (for more details, see (13)).

4.2 Performance Criteria

Table 3: Summary of performance criteria metrics for all three test vehicles when state feedback controllers are implemented on lane change and roundabout manoeuvres. TST = Tractor-Semitrailer; BD = B-double; BT = B-triple.

Manoeuvre	Roundabout			Lane Change		
Weighting (w)	5			5		
Vehicle (n)	TST (1)	BD (2)	BT (3)	TST (1)	BD (2)	BT (3)
Axle offset RMS [m]	0.027	0.050	0.135	0.020	0.034	0.128
Axle offset max [m]	0.085	0.137	0.389	0.059	0.112	0.321
Steer integral [radm]	19.71	18.85	22.24	5.66	8.75	23.80
RMS steer rate [deg/m]	2.60	3.65	8.08	1.26	1.90	6.44
Swept path RMS [m]	4.46	6.36	11.97	2.83	3.51	7.22
Swept path max [m]	6.06	8.80	15.47	3.59	5.26	10.56

The experimental results for all three test vehicles on both paths, in terms of the performance criteria outlined in Section 2.2, are shown in Table 3. These metrics were calculated individually for each run and then averaged for the three repeats, to avoid any biasing effect of averaging the time histories. The performance metrics all show an increase with the number of trailers on both paths, as would be expected. An exception is the steer integral for the Tractor-Semitrailer on the roundabout path, which is higher than the value for the B-double. This is because the steady-state front axle steer angle is higher for this case, due to the smaller radius of the tractor unit. This exception has no significance in terms of controller performance.

In most cases, the performance metrics worsen slightly when comparing the B-double to the Tractor-Semitrailer. There is, however, a significant reduction in performance when the B-triple combination is evaluated. The RMS equivalent axle offsets of the B-double are less than double those of the Tractor-Semitrailer. The RMS equivalent axle offsets of the B-triple are a factor of approximately 3 to 4 worse than the B-double. This is also seen on the RMS steer rate, which shows a 40-50% increase when comparing the Tractor-Semitrailer and B-double and a 120-240% increase when comparing the B-double and B-triple.

In all cases, the path-tracking performance is considered to be sufficiently accurate as to be applicable in a practical implementation of this technology.

5 Conclusions

(i) A general path-tracking controller has been implemented on full-size HGVs with one, two and three trailers.

(ii) The path-tracking controller presented in this paper can be used to control the path of the rear end of an articulated vehicle with one, two or three trailers with a path error of less than 400mm in all cases. This is thought to be sufficiently accurate for practical implementation.

(iii) All aspects of path-tracking controller performance worsen as the number of trailers increases. This is most significant for the B-triple (three trailers).

(iv) All experimental results show the presence of small steady-state oscillations (less than one tyre width), which increase with the number of trailers. These are due to a closed-loop system pole being driven by vehicle disturbances.

6 Figures

Figure 1: The test vehicles: (a) Tractor-Semitrailer, (b) B-double and (c) B-triple. The Denby 'Extra' Eco-Link B-trailer was loaned by Denby transport. All other vehicle units are part of the CVDC test vehicle fleet. Distances shown between the front axle and the hitch point for the tractor unit, hitch to hitch for B-trailers and hitch to equivalent rear axle for the tanker.

Figure 2: Vehicle model schematic, shown here for a two-trailer vehicle. (Definitions of dimensions in Table 1 and Nomenclature section)

Figure 3: Vehicle diagram illustrating state feedback controller, for a two-trailer vehicle

Figure 4: Control loop for state feedback controller shown for the general n-trailer case. Here, κ denotes the curvature of the path.

Figure 5: Damping ratio variation with weighting, w, for B-trains with n trailers when path tracking controller is used (tuned using LQR)

Figure 6: Diagram of test equipment for B-double test vehicle (vehicles separated for clarity)

Figure 7: Block diagram representing global controller software code. The implementation of the 'controller' is the path-tracking state feedback controller.

Figure 8: Lane change manoeuvre showing the measured positions of the equivalent axle of the rear trailer for all three test vehicles, when state feedback control is used. On this plot, the width of the path is 1m.

Figure 9: Roundabout manoeuvre showing the measured positions of the equivalent axle of the rear trailer for all three test vehicles, when state feedback control is used. On this plot, the width of the path is 1m.

Figure 10: Comparison of Tractor-Semitrailer (TST), B-double (BD) and B-triple (BT) vehicle testing measurements for state feedback controller on gentle lane change path for a weighting (w) of 5, showing (a) offsets of the equivalent axle on the rear trailer, (b) front axle steer angle, (c) heading offsets of the equivalent axle, (d) last articulation angle, (e) penultimate articulation angle and (f) first articulation angle (for the B-triple).

Figure 11: Comparison of Tractor-Semitrailer (TST), B-double (BD) and B-triple (BT) vehicle testing measurements for state feedback controller on roundabout path for a weighting (w) of 5, showing (a) offsets of the equivalent axle on the rear trailer, (b) front axle steer angle, (c) heading offsets of the equivalent axle, (d) last articulation angle, (e) penultimate articulation angle and (f) first articulation angle (for the B-triple).

Figure A1: General vehicle model showing (a) tractor unit and (b) a general trailer – free body diagrams

7 Acknowledgment

This research was funded by the Engineering and Physical Sciences Research Council (EPSRC) and Volvo Trucks through an Industrial CASE award. The authors would like to acknowledge Leo Laine and Carl-Johan Hoel from Volvo Trucks for their collaboration and contributions to the research.

The authors would like to acknowledge Denby Transport for their loan of the 'Extra' Eco-Link B-trailer for use in vehicle testing.

The authors would like to acknowledge the members of the CVDC who supported the work in this paper. At the time of writing, the Consortium consisted of the University of Cambridge with the following partners from the heavy vehicle industry: Anthony Best Dynamics, Camcon, Denby Transport, Firestone Air Springs, GOODYEAR DUNLOP, Haldex, Motor Industry Research Association, SDC Trailers, SIMPACK, Tinsley Bridge, Tridec, Volvo Trucks, and Wincanton.

8 Nomenclature

a	Distance from CoG to front axle of tractor unit or front hitch point of trailer [m]
b	Distance from CoG to rear axle of tractor unit or first axle of trailer [m]
d	Width of vehicle unit [m]
c	Distance from rear axle of tractor unit or first axle of trailer to rear hitch point [m]
e	Distance between adjacent axles on trailers [m]
f_d	Ordinary differential equation function for dynamic vehicle model
f_m	Equations of motion function for dynamic vehicle model
fo	Distance from front axle or front hitch point to front of vehicle unit [m]
h	Distance from leading hitch point to rear hitch point on trailer [m]

l	Equivalent wheelbase of vehicle unit [m]
m	Mass of vehicle unit [kg]
n	Number of trailers
n_a	Number of axles on vehicle unit
ro	Distance from rear axle of tractor unit or first axle of trailer to rear of vehicle unit[m]
s	Distance along the path [m]
u	Longitudinal velocity of vehicle unit [m/s]
v	Lateral velocity of vehicle unit at the rear axle for the kinematic model or at the CoG for the dynamic model [m/s]
w	Cost function weighting
y_a	Lateral offset of the equivalent axle of the rear trailer to the desired path [m]
z	State vector of vehicle model
C_1	Tyre cornering coefficient [rad^{-1}]
C_2	Tyre curvature coefficient [$N^{-1}rad^{-1}$]
F	Lateral tyre force [N]
I	Yaw moment of inertia of vehicle unit, about the CoG [kgm^2]
J	Cost function for controller tuning

K	Controller gain
L_{LA}	Look-ahead distance for state feedback controller [m]
P_A	Equivalent axle of rear trailer point on path
P_L	Look-ahead point on path
V_A	Equivalent axle of rear trailer
X	Longitudinal hitch force at the rear hitch of the vehicle unit [N]
Y	Lateral hitch force at the rear hitch of the vehicle unit [N]
Z	Vertical tyre force [N]
α	Tyre sideslip angle [rad]
δ	Tractor unit front axle steer angle [rad]
ζ	Damping ratio of closed-loop linear system
θ	Heading angle of vehicle unit [rad]
θ_p	Heading angle of path [rad]
μ	Coefficient of friction between the tyre and the road surface
Γ	Articulation angle [rad]
Ω	Yaw angular velocity [rad/s]
$[\mathbf{A}]$	Closed-loop system matrix

[**H**] Linear vehicle model equations of motion matrix

[**K**] Linear gain matrix

[**M**] Linear vehicle model equations of motion matrix

[**N**] Linear vehicle model equations of motion matrix

Subscripts and Superscripts

$\dot{}$ First derivative with respect to time

$\ddot{}$ Second derivative with respect to time

a The addition of observer states in the vehicle model

e Equilibrium value

f Front axle

i Corresponding to i^{th} vehicle unit

j Corresponding to articulation joint between j^{th} and $j+1^{th}$ vehicle unit

n Corresponding to the last articulation joint

r Rear axle

t_i Axle of i^{th} trailer

y Corresponding to the lateral path error

Γ Corresponding to the articulation angle error

9 Appendix: Vehicle Model Equations of Motion

A tractor unit with n trailers has n+1 units. Index 'i' is used to denote the unit number, where i = 1 is used for the tractor unit, i = 2 for the first trailer etc.

From Figure A1(b), it can be seen that for all trailers (i = 2, 3,..., n+1), the moments of each trailer about the leading hitch point can be calculated from:

$$I_i\dot{\Omega}_i - m_i(\dot{v}_i + u_i\Omega_i)a_i - F_{t_i}(a_i + b_i) + Y_i(a_i + b_i + c_i) = 0 \quad \text{(A.1)}$$

Here, I_i and m_i are the yaw inertia and mass, u_i, v_i and Ω_i are the longitudinal velocity, lateral velocity and yaw rate at the centre of mass and $\dot{u}_i$, $\dot{v}_i$ and $\dot{\Omega}_i$ are their derivatives. F_{t_i} are the lateral tyre forces. a_i, b_i and c_i are front axle to CoG, CoG to rear axle and rear axle to hitch distances, as shown in Figure 2 ($l = a_{n+1} + b_{n+1}$). Y_i is the lateral hitch force at the rear hitch of the i^{th} vehicle unit.

To enable moments of the vehicle unit ahead to be calculated, the coupling forces at the rear hitch point, perpendicular and parallel to each trailer are required:

$$Y_{i-1} = \left(Y_i - m_i(\dot{v}_i + u_i\Omega_i) - F_{t_i}\right)\cos(\Gamma_{i-1}) - \left(X_i + m_i(\dot{u}_i - v_i\Omega_i)\right)\sin(\Gamma_{i-1}) \quad \text{(A.2)}$$

$$X_{i-1} = \left(Y_i - m_i(\dot{v}_i + u_i\Omega_i) - F_{t_i}\right)\sin(\Gamma_{i-1}) + \left(X_i + m_i(\dot{u}_i - v_i\Omega_i)\right)\cos(\Gamma_{i-1}) \quad \text{(A.3)}$$

where X_i is the longitudinal hitch force at the rear hitch of the i^{th} vehicle unit.

Balancing the lateral forces on the tractor unit:

$$m_1(\dot{v}_1 + u_1\Omega_1) + F_f\cos(\delta) + F_r - Y_1 = 0 \quad \text{(A.4)}$$

where F_f and F_r are the lateral tyre forces on the tractor unit front and rear axles.

The moments of the tractor unit about its hitch point can also be calculated:

$$m_1(\dot{v}_1 + u_1\Omega_1)(b_1 + c_1) + F_f \cos(\delta)(a_1 + b_1 + c_1) + F_r c_1 + I_1\dot{\Omega}_1 = 0 \quad (A.5)$$

With the addition of calculations of the sideslip angles of the tyres and the lateral tyre force model (Equations 1 and 2), these equations are sufficient to calculate the motion of the vehicle in forward or reverse directions.

10 References

1. Odhams AMC, Roebuck RL, Lee YJ, Hunt SW, Cebon D. Factors influencing the energy consumption of road freight transport. Proceedings of the Institution of Mechanical Engineers, Part C: Journal of Mechanical Engineering Science. 2010;224(9):1995-2010.

2. Woodrooffe J, Ash L. Economic Efficiency of Long Combination Transport Vehicles in Alberta. Woodrooffe and Associates, Canada: Prepared for Alberta Infrastructure, 2001.

3. Kjell M, Westerlund KR. Feasibility of Longer Combination Vehicles. Göteborg, Sweden: Chalmers University of Technology; Dissertation submitted for the degree of Masters, 2009.

4. Michalek M, editor. Geometrically motivated set-point control strategy for the standard N-trailer vehicle. Proceedings of the Intelligent Vehicles (IV) Symposium; 2011; Baden-Baden, Germany.

5. Matsushita K, Murakami T. Backward Motion Control for Articulated Vehicles with Double Trailers Considering Driver's Input. Proceedings of the IEEE International Conference on Industrial Electronics (IECON); 2006; Paris, France.

6. Morales J, Martinez JL, Mandow A, Garcia-Cerezo AJ. Steering the Last Trailer as a Virtual Tractor for Reversing Vehicles With Passive On- and Off-Axle Hitches. IEEE Transactions on Industrial Electronics. 2013;60(12):5729-36.

7. Morales J, Mandow A, Martínez J, Reina A, García-Cerezo A. Driver Assistance System for Passive Multi-Trailer Vehicles with Haptic Steering Limitations on the Leading Unit. Sensors. 2013;13(4):4485-98.

8. Sekhavat S, Lamiraux F, Laumond JP, Bauzil G, Ferrand A. Motion planning and control for Hilare pulling a trailer: experimental issues. Proceedings of the IEEE International Conference on Robotics and Automation (IRCA); 1997; Albuquerque, New Mexico.

9. Michałek MM. A highly scalable path-following controller for N-trailers with off-axle hitching. Control Engineering Practice. 2014;29:61-73.

10. Tanaka K, Taniguchi T, Wang HO, editors. Trajectory control of an articulated vehicle with triple trailers. Proceedings of the IEEE International Conference on Control Applications; 1999; Hawaii.

11. Bolzern P, DeSantis RM, Locatelli A, Masciocchi D. Path-tracking for articulated vehicles with off-axle hitching. IEEE Transactions on Control Systems Technology. 1998;6(4):515-23.

12. Bolzern P, DeSantis RM, Locatelli A. An Input-Output Linearization Approach to the Control of an n-Body Articulated Vehicle. Journal of Dynamic Systems, Measurement and Control, Transactions of the ASME. 2001;123(3):309-16.

13. Rimmer AJ. Autonomous Reversing of Multiply-Articulated Heavy Vehicles. University of Cambridge; Dissertation submitted for the degree of Doctor of Philosophy, 2014.

14. Winkler CB. Simplified Analysis of the Steady-State Turning of Complex Vehicles. Vehicle System Dynamics. 1998;29(3):141-80.

15. Gillespie TD. Fundamentals of Vehicle Dynamics. Warrendale, Pennsylvania: Society of Automotive Engineers; 1992. 495 p.

16. Pacejka HB. Tyre and Vehicle Dynamics. Oxford: Butterworth-Heinemann; 2012.

17. Fancher P. A factbook of the mechanical properties of the components for single-unit and articulated heavy trucks. University of Michigan Transportation Research Institute (UMTRI) 1986.

18. Jujnovich BA. Active Steering of Articulated Vehicles. Dissertation submitted for the degree of Doctor of Philosophy, University of Cambridge; 2005.

19. Cheng C. Enhancing Safety of Actively-Steered Articulated Vehicles. Dissertation submitted for the degree of Doctor of Philosophy, University of Cambridge; 2009.

20. Anon. Cambridge Vehicle Dynamics Consortium (CVDC) Homepage. Department of Engineering, University of Cambridge2014 [01/08/2014]; Available from: http://www-cvdc.eng.cam.ac.uk/.

21. Franklin GF, Powell DJ, Emami-Naeini A. Feedback Control of Dynamic Systems. Englewood Cliffs, New Jersey: Prentice Hall PTR; 2001. 912 p.

22. Anderson BDO, Moore JB. Linear Optimal Control. Newcomb RW. Englewood Cliffs, New Jersey: Prentice Hall; 1971.

23. Altafini C, Speranzon A, Wahlberg B. A feedback control scheme for reversing a truck and trailer vehicle. IEEE Transactions on Robotics and Automation. 2001;17(6):915-22.

24. Larsson U, Zell C, Hyyppa K, Wernersson A. Navigating an articulated vehicle and reversing with a trailer. Proceedings of the IEEE International Conference on Robotics and Automation (IRCA); 1994; San Diego, California.

25. Anon. V.S.E. Vehicle Systems Engineering B.V. Homepage. 2014 [01/08/2014]; Available from: http://www.v-s-e.com/en.

26. Anon. Product information ETS for trailers. In: Engineering VS.

27. Anon. RT Inertial and GPS Measurement Systems: User Guide. In: Ltd. OTS, 2010.

28. Anon. Steering Robot SR Series User Guide. Anthony Best Dynamics Ltd., 2012.

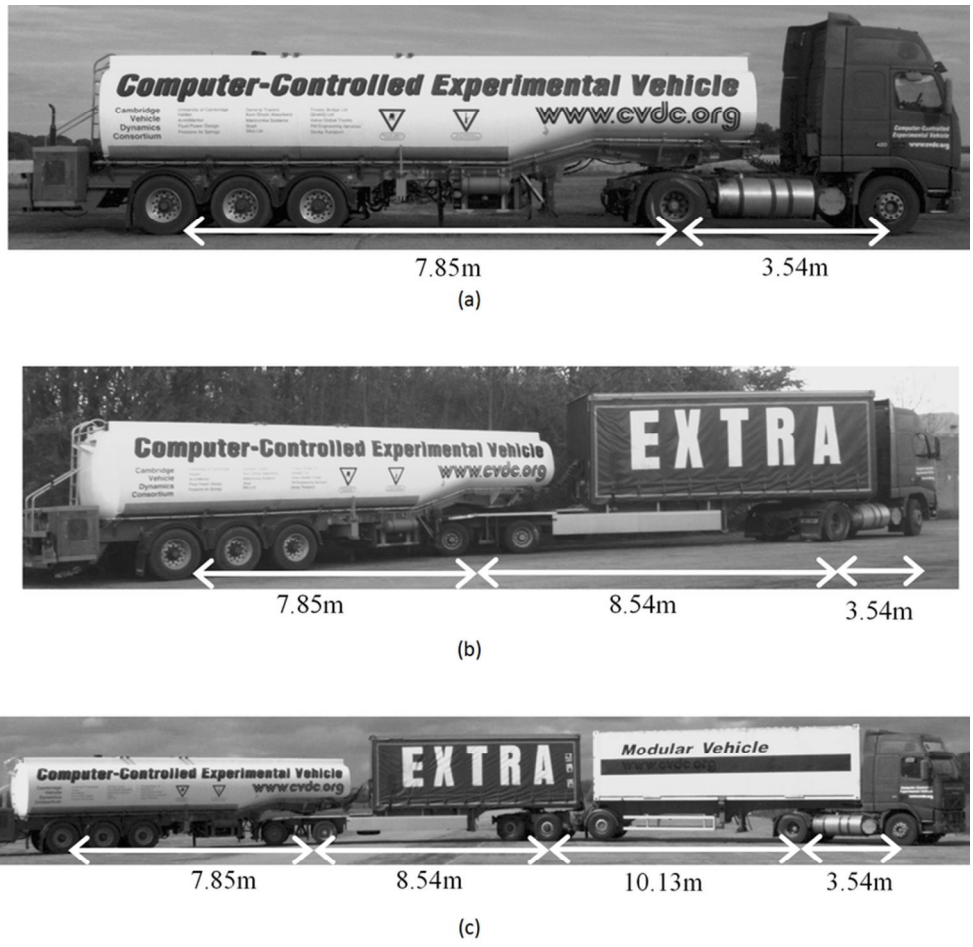

Figure 1: The test vehicles: (a) Tractor-Semitrailer, (b) B-double and (c) B-triple. The Denby 'Extra' Eco-Link B-trailer was loaned by Denby transport. All other vehicle units are part of the CVDC test vehicle fleet. Distances shown between the front axle and the hitch point for the tractor unit, hitch to hitch for B-trailers and hitch to equivalent rear axle for the tanker.
76x73mm (300 x 300 DPI)

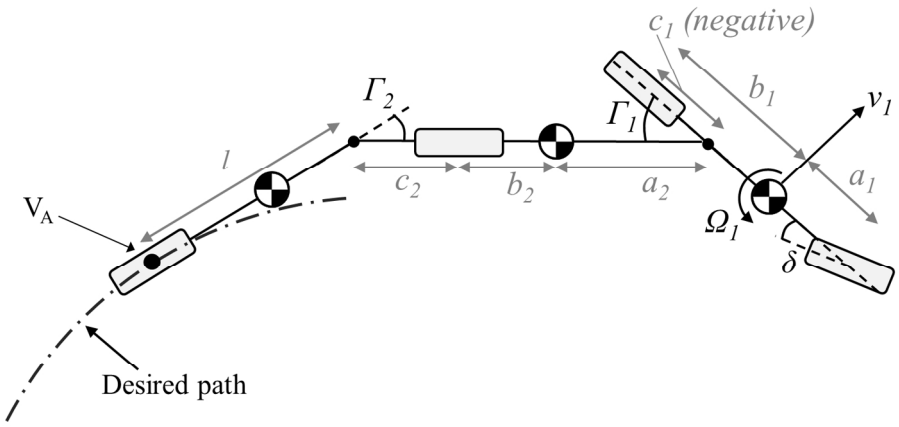

Figure 2: Vehicle model schematic, shown here for a two-trailer vehicle. (Definitions of dimensions in Table 1 and Nomenclature section)
297x146mm (150 x 150 DPI)

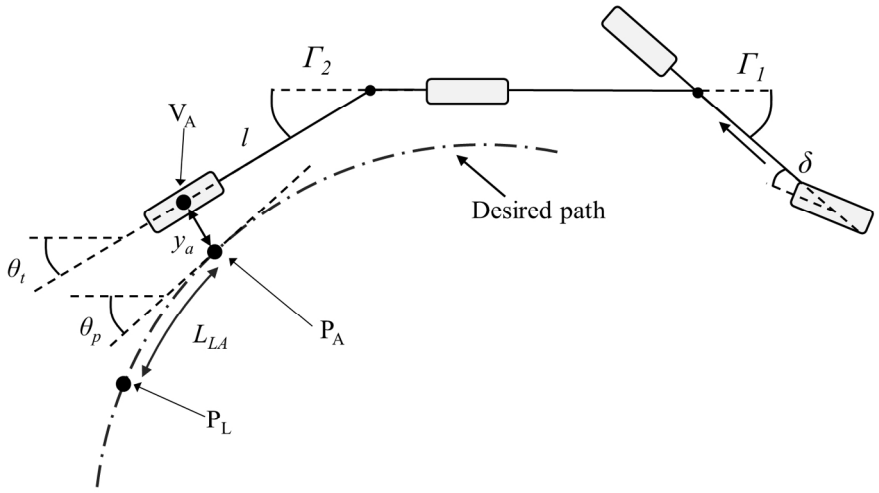

Figure 3: Vehicle diagram illustrating state feedback controller, for a two-trailer vehicle
321x199mm (150 x 150 DPI)

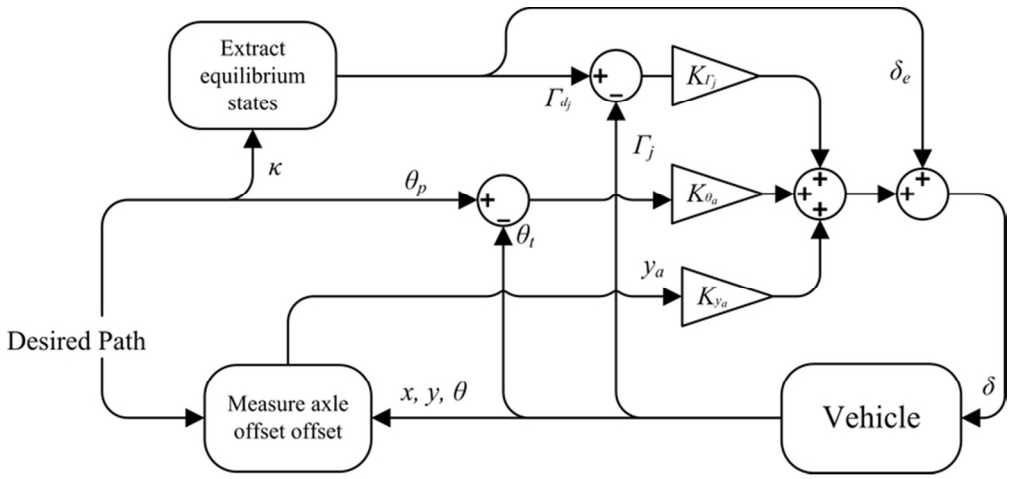

Figure 4: Control loop for state feedback controller shown for the general n-trailer case. Here, κ denotes the curvature of the path.
72x34mm (300 x 300 DPI)

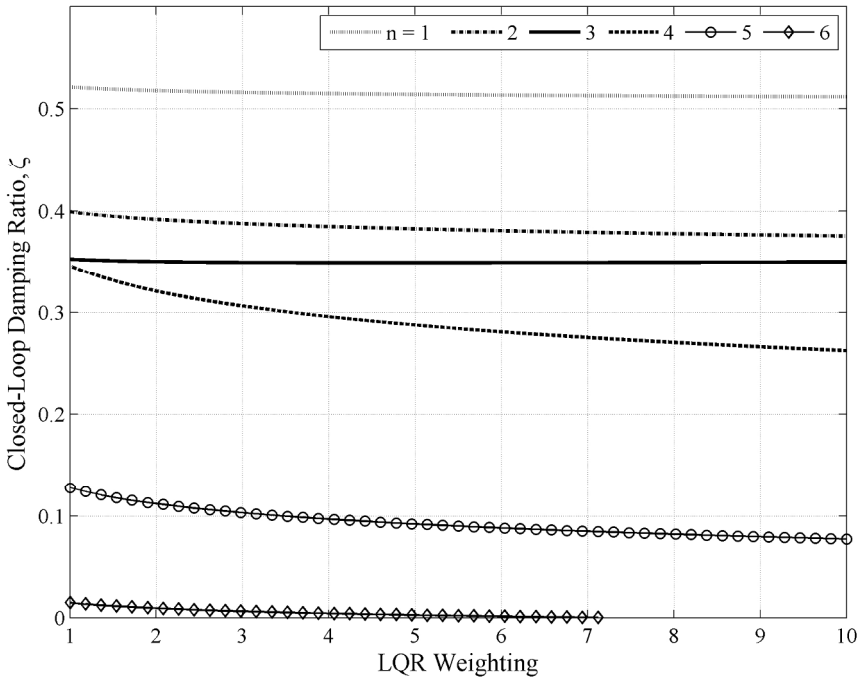

Figure 5: Damping ratio variation with weighting, w, for B-trains with n trailers when path tracking controller is used (tuned using LQR)
203x152mm (300 x 300 DPI)

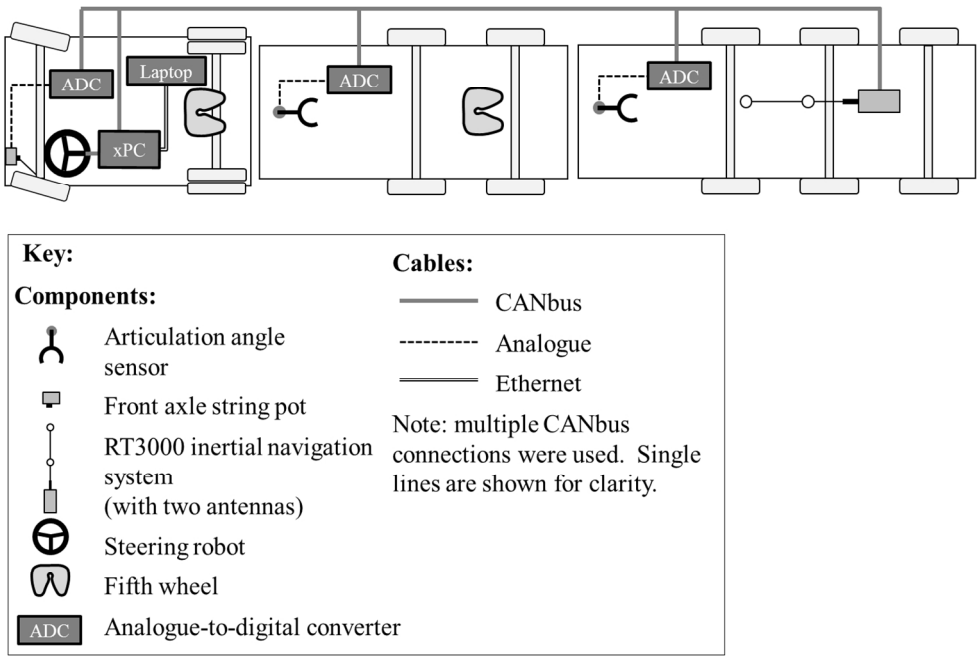

Figure 6: Diagram of test equipment for B-double test vehicle (vehicles separated for clarity)
254x173mm (150 x 150 DPI)

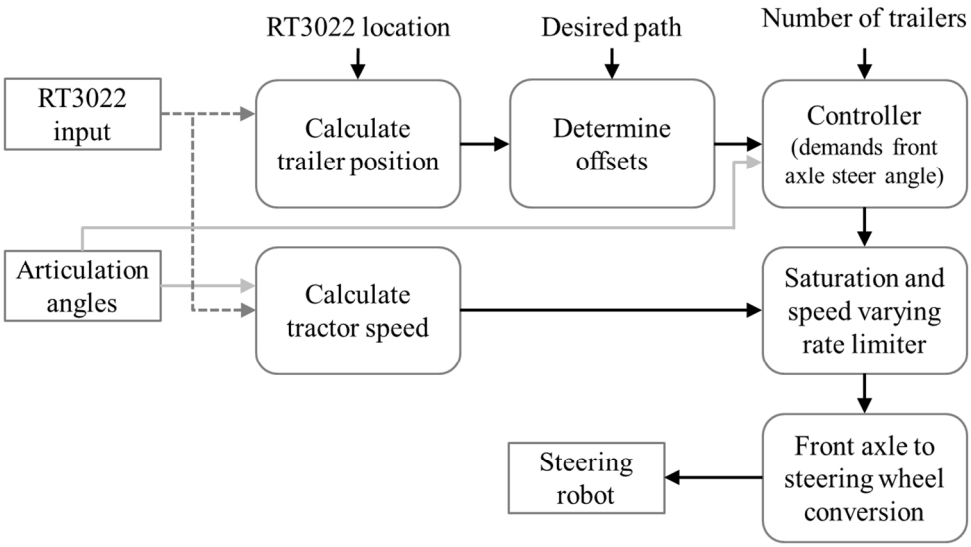

Figure 7: Block diagram representing global controller software code. The implementation of the 'controller' is the path-tracking state feedback controller.
230x134mm (150 x 150 DPI)

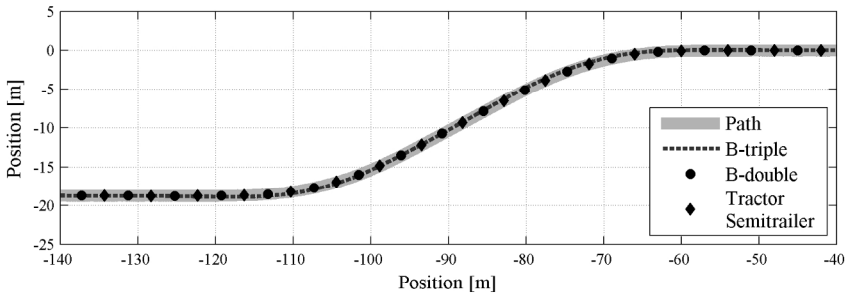

Figure 8: Lane change manoeuvre showing the measured positions of the equivalent axle of the rear trailer for all three test vehicles, when state feedback control is used. On this plot, the width of the path is 1m.
180x120mm (300 x 300 DPI)

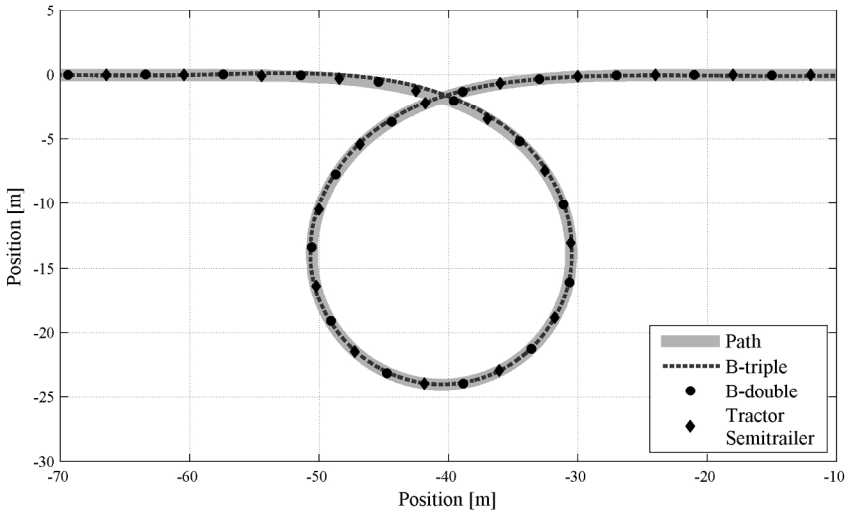

Figure 9: Roundabout manoeuvre showing the measured positions of the equivalent axle of the rear trailer for all three test vehicles, when state feedback control is used. On this plot, the width of the path is 1m.
180x120mm (300 x 300 DPI)

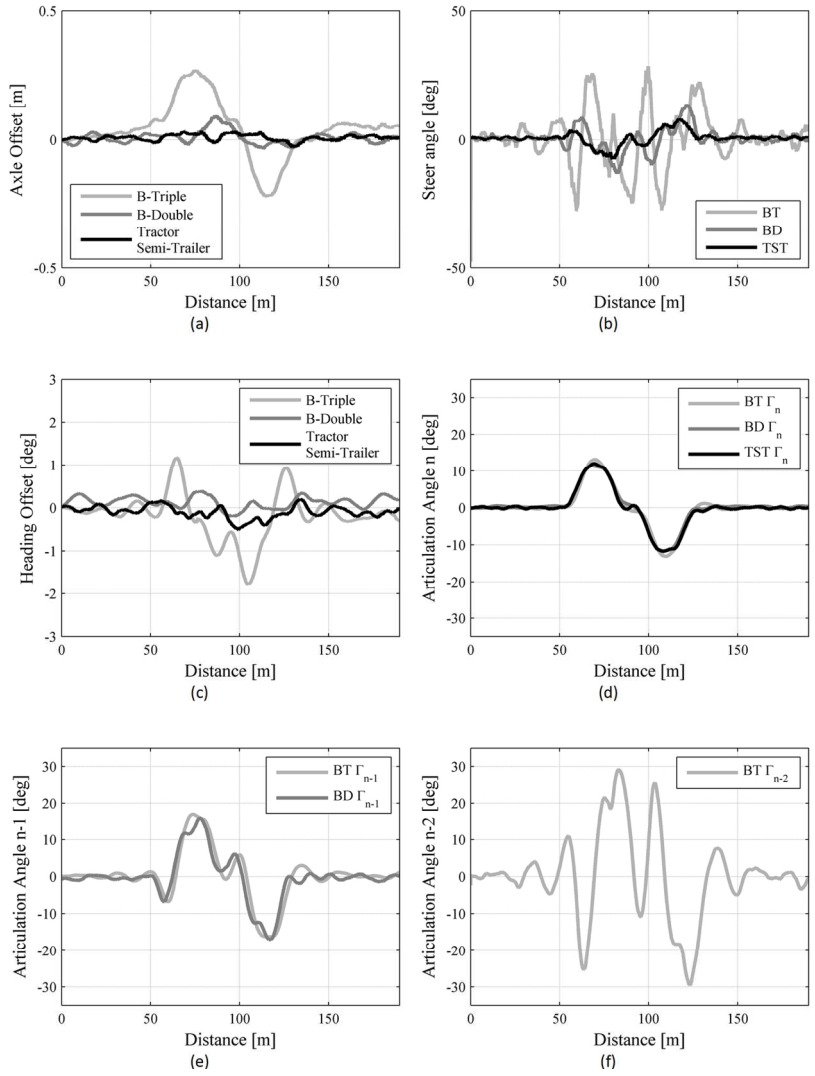

Figure 10: Comparison of Tractor-Semitrailer (TST), B-double (BD) and B-triple (BT) vehicle testing measurements for state feedback controller on gentle lane change path for a weighting (w) of 5, showing (a) offsets of the equivalent axle on the rear trailer, (b) front axle steer angle, (c) heading offsets of the equivalent axle, (d) last articulation angle, (e) penultimate articulation angle and (f) first articulation angle (for the B-triple).
120x176mm (300 x 300 DPI)

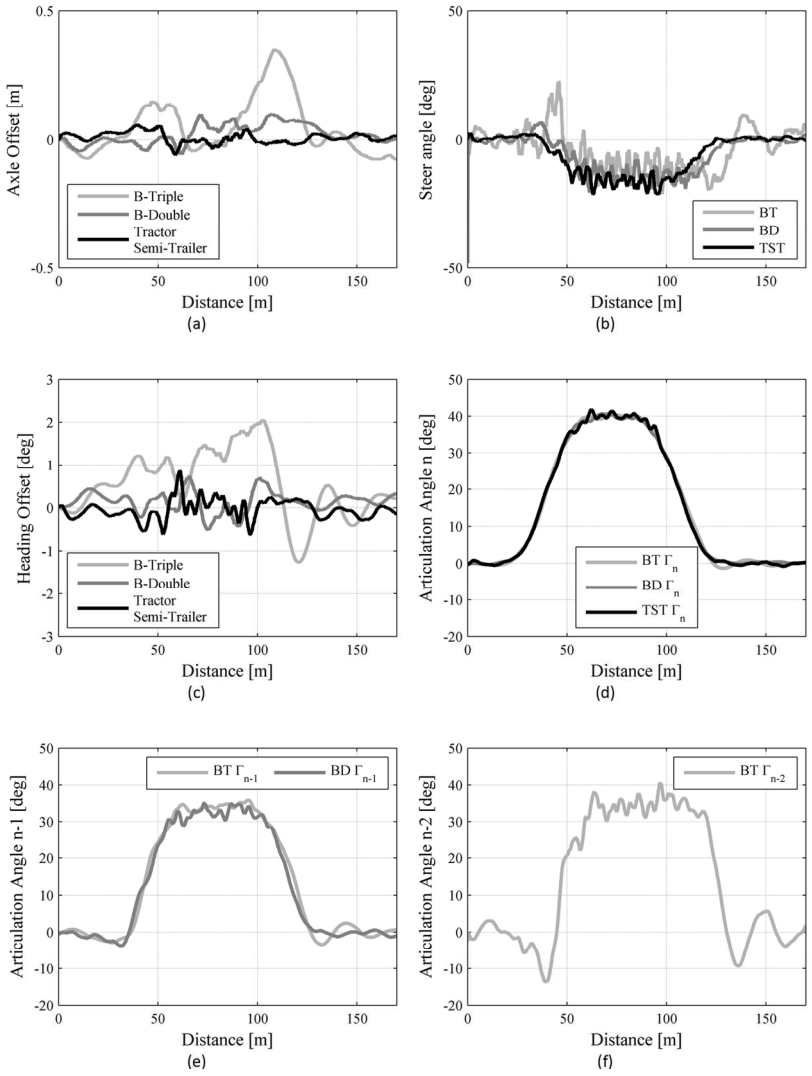

Figure 11: Comparison of Tractor-Semitrailer (TST), B-double (BD) and B-triple (BT) vehicle testing measurements for state feedback controller on roundabout path for a weighting (w) of 5, showing (a) offsets of the equivalent axle on the rear trailer, (b) front axle steer angle, (c) heading offsets of the equivalent axle, (d) last articulation angle, (e) penultimate articulation angle and (f) first articulation angle (for the B-triple).
120x176mm (300 x 300 DPI)

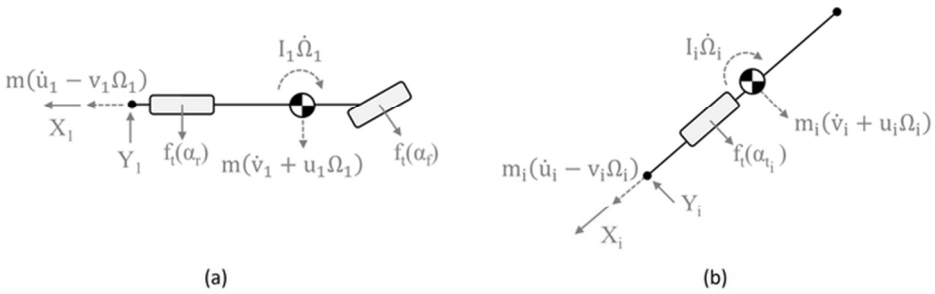

Figure A1: General vehicle model showing free body diagrams: (a) tractor unit and (b) a general trailer
65x26mm (300 x 300 DPI)